

# Polar Order by Rational Design: Crystal Engineering with Parallel Beloamphiphile Monolayers<sup>†</sup>

RAINER GLASER\*

Department of Chemistry, University of Missouri–Columbia, Columbia, Missouri 65211

Received November 1, 2005

**ABSTRACT**

Polar order in the biosphere is limited to nanometer-sized domains, occurs with essentially complete cancellation, or is avoided on purpose. One thus wonders whether large-scale polar order is even possible, and this question is the subject of the dipole alignment problem. We addressed this challenge with an interdisciplinary approach bringing together elements of mathematics, electronic structure theory and computational chemistry, physical-organic and synthetic chemistry, crystallization and crystallography, and, most importantly, patience and much thought about intermolecular bonding in molecular crystals. The azine- and biphenyl-based beloamphiphiles ( $Y\text{-Ph-MeC=N-N=CMe-Ph-X}$  and  $Y\text{-Ph-Ph-X}$ ) are ascendants of a new generation of highly anisotropic functional materials with perfect polar order.

*“It is very hard to be a rational designer; even faking that process is quite difficult. However, the result is a product that can be understood, maintained, and reused. If the project is worth doing, the methods described here are worth using.”* — Parnas and Clements, 1986.

**Introduction**

Proteins have evolved for 3–4 billion years into an enormous array of structural diversity and function.<sup>1,2</sup> While  $\beta$ -sheets feature dipole cancellation, the  $\alpha$  helix shows one-dimensional dipole-parallel alignment and thus provides the potential for highly polar tertiary structures. Yet, polar alignment is not realized beyond small domains (parallel coiled coils,  $\alpha,\beta$ -barrels), and one wonders whether high polar alignment is not attainable in principle or whether it is merely difficult to find a natural way for its realization.

It has been our goal to explore the question “Is it possible to aggregate dipolar molecules in condensed phase in such a way that all molecular dipole moments are parallel aligned?” This dipole-alignment problem presents a grand challenge,<sup>3,4</sup> and many wrote that the problem cannot be solved. In this Account we present an

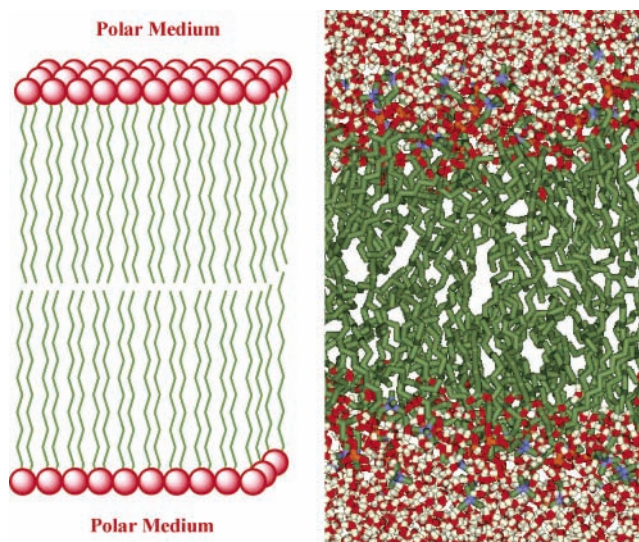


**FIGURE 1.** Idea of a lipid bilayer, and snapshot of a dipalmitoylphosphatidylcholine (DPPC) lipid membrane simulation.

analysis of the challenge and show how this analysis has led to the realization of crystalline materials with large-scale polar order with a rational approach that involves “polar stacking of polar bolaamphiphile monolayers”.

Lipid bilayers feature two-dimensional dipole-parallel alignment in each monolayer. Because lipid bilayers “naturally” contain oppositely oriented polar monolayers, one might never consider lipid bilayers as potential sources for the construction of high degrees of polarity. Yet, a better understanding of lipid bilayers actually provides a guide to polar materials and begins with the realization of the deep chasm between chemists’ typical ideas of nicely organized layers and the reality of lipid bilayers as exhibited in Figure 1.<sup>5,6</sup> Two insights that are particularly important here concern the nature of the lateral interactions in lipid bilayers and the role of solvation for the opposite orientation of the two monolayers. While amphiphile monolayers can be highly ordered,<sup>7,8</sup> the monolayers in lipid bilayers often are rather fluid and there is little lateral interaction.<sup>9</sup> The lipid bilayer energetics in water is largely driven by the desire of the polar head groups to interact with each other and with water,<sup>10,11</sup> and solvation of the head groups is a major reason for the opposite orientation of the two polar layers.

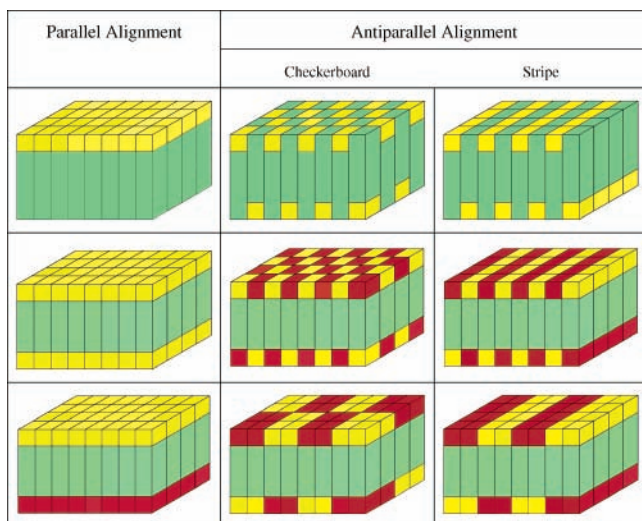
## Amphiphiles, Idioteloamphiphiles, Belaamphiphiles, and Beloamphiphiles

**Amphiphile Monolayers.** Amphiphiles (Greek, *amphibios*) are “living a double life” by combination of a polar and water-soluble head group (yellow) and a nonpolar and water-insoluble alkyl chain (green). Some important types of amphiphile monolayers are shown in Scheme 1.

Rainer Ernst Glaser studied chemistry and physics in Tübingen (Dipl.-Chem. 1984), Berkeley, CA (M.S. 1983, Ph.D. 1987), and New Haven, CT (postdoctoral 1987–1989). He joined the faculty at the University of Missouri–Columbia in 1989 and is now Professor in Chemistry. His research includes topics in organic, theoretical, and materials chemistry, chemistry education, and astronomy; he has collaborated with chemists, biochemists, physicists, mathematicians, journalists, and educators. He was a Fellow of the Studienstiftung des Deutschen Volkes 1981–1984, a Fulbright Fellow 1982–1983, a Predoctoral Fellow of the Fonds der Chemischen Industrie 1985–1987, a JSPS Postdoctoral Fellow in 1997 and elected AAAS Fellow in 2004 and Fellow of the RSC in 2006.

\* To whom correspondence should be addressed. E-mail: glaser@missouri.edu.

<sup>†</sup> Dedicated to Johanna Glaser on the occasion of her 70th birthday.

Scheme 1. Types of Amphiphile Monolayers (AM)<sup>a</sup>

<sup>a</sup> In the top row are shown a parallel amphiphile monolayer (PAM) and two types of antiparallel amphiphile monolayers (APAM). Below the PAM are shown an idioteloamphiphile monolayer (IAM) and a parallel beloamphiphile monolayer (PBAM). In addition, four types of antiparallel beloamphiphile monolayers (APBAM) are shown.

The monolayers are classified as “symmetrical” or “unsymmetrical” depending on whether all amphiphiles are oriented in the same direction (parallel) or whether their orientations alternate (antiparallel) in at least one direction. While there is *one* symmetrical monolayer, unsymmetrical monolayers can be constructed *in a great many ways*, and the checkerboard and stripe motifs are common. Idioteloamphiphiles contain two polar head groups of the same kind (Greek, *idios*) at the ends (Greek, *telos*) of a nonpolar chain. Bolaamphiphiles contain different head groups at the ends of a usually saturated hydrocarbon spacer. The term is derived from the name of a hunting tool that consists of weights attached to the end of a string (Spanish, *bolos*). Beloamphiphiles are polar and conjugated bolaamphiphiles, and the prefix *belo* (Greek, *belos*, arrow) reflects that beloamphiphiles have dipole moments. In particular, symmetrically D–D and A–A disubstituted (conjugated) molecules are idioteloamphiphiles, and unsymmetrically D–A, D1–D2, and A1–A2 disubstituted (conjugated) molecules are beloamphiphiles. In the terminology of monolayers, the terms “symmetrical” and “unsymmetrical”, respectively, are commonly used to describe the amphiphile alignment in the same or alternating directions, respectively. This practice causes confusion in discussions of “symmetrical monolayers” formed by “unsymmetrical molecules”, and we prefer to characterize the amphiphile monolayer alignment as “parallel” or “antiparallel.”

**Parallel Amphiphile Monolayers, Micelles, and Liposomes.** Parallel amphiphile monolayers (PAMs) are best known for their formation of micelles (monolayer lipid membrane vesicles, MLMV), and micelle science has greatly evolved from early lipid micelles<sup>12</sup> to polymer–amphiphile micelles.<sup>13</sup> PAMs may curl up in only one dimension to form micellar rods, and cone-shaped peptide amphiphiles were reported to form cylindrical PAM nanofibers.<sup>14</sup> Formation of polar layers of mushroom

bundles<sup>15</sup> also was considered, but the initial claim has not been substantiated.

Bilayers consisting of two parallel amphiphile monolayers *always* feature oppositely oriented PAMs, and they form lipid bilayers,<sup>16</sup> fibers,<sup>17</sup> and liposomes<sup>18</sup> (lipid membrane vesicles, LMVs). Nonlipid amphiphiles also form spherical liposomes<sup>19</sup> as well as liposomal rods and nanofibers.<sup>20</sup>

**Polar Order in Amphiphile Crystals.** The majority of layer-forming amphiphiles crystallize with alternating orientation in both layer directions (checkerboard), and even polar alignment in one layer direction (stripe) is rare.<sup>21</sup> Polar order throughout an amphiphile monolayer apparently was first observed by Sim in 1955 in crystals of 11-aminoundecanoic acid hydrobromide hemihydrate ( $\text{Br}^- \cdot \text{H}_3\text{N}-(\text{CH}_2)_{10}-\text{COOH} \cdot 0.5\text{H}_2\text{O}$ ).<sup>22</sup> Crystals of Sim’s acid contain “normal bilayers” and are overall nonpolar.

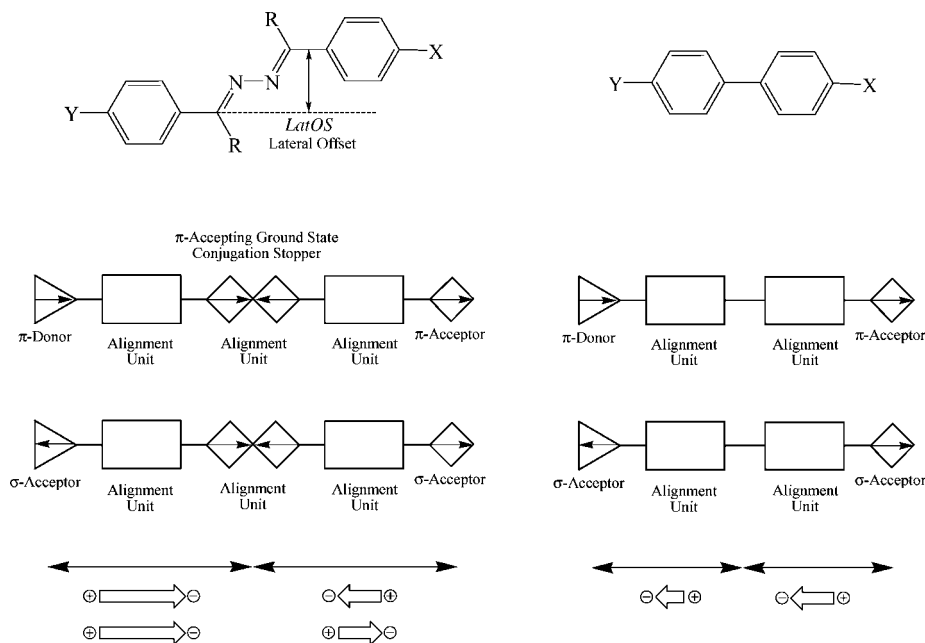
The crystal structures of three alkyl gluconamides ( $\text{C}_n\text{H}_{2n+1}-\text{NH}-\text{CO}-(\text{CHOH})_4-\text{CHOH}$ ,  $n = 7,^{23} 8,^{23} 11^{24}$ ) and one galactosamide (galactose– $\text{NH}-\text{CO}-(\text{CH}_2)_{14}-\text{COOH}$ )<sup>25</sup> apparently present the first cases of polar stacking of polar bolaamphiphile monolayers. These cases remain unexplained, and many similar amphiphiles crystallize without overall polarity.

## Polar Order by Rational Design

Since collinear dipoles will align parallel, three-dimensional polar order depends on the question of whether dipole-parallel alignment can be achieved in the second and third dimensions. We met the challenge with a solution that consists in the creation of two-dimensional layers with polarity perpendicular to the layer surfaces and their polar stacking in the third dimension. Specifically, the beloamphiphile monolayers (BAM) are comprised of molecules whose long axes and dipole moment vectors are more or less aligned with each other and perpendicular to the layer surfaces, i.e. the thickness of a BAM is close to the length of its constituents. These two-dimensional BAMs need to be distinguished and are not to be confused with two-dimensional sheets, that is, an arrangement of molecules whose long axes lie more or less in a common plane.

**Fundamental Insight Shapes Basic Strategy.** We began with studies of the energies of point dipole lattices, and in the mid-1990’s we made a discovery of fundamental significance:<sup>26,27</sup> As expected, antiparallel alignment is always preferred over the parallel-aligned lattice, but the latter might be a local minimum! This paradigm-shifting discovery placed the grand challenge in an entirely different light; a systematic solution of the dipole-alignment problem was possible in principle. The study also provided guidance. First, the molecular dipoles should be modest so that parallel alignment can compete with antiparallel alignment. Second, the dipolar molecules need to be designed for large lateral attraction so that a pair of side-by-side dipolar molecules will be either parallel or antiparallel but not in an arrangement that is neither.

**Scheme 2. Beloamphiphile Design for Achievement of Polar Stacking of Parallel Beloamphiphile Monolayers (PBAMs): Azines  $Y-Ph-MeC=N-N=CMe-Ph-X$  and Biphenyls  $Y-Ph-Ph-X$**



Third, dipolar molecules need to be designed so that the lateral attractions stabilize the polar lattice more than any nonpolar lattice. These ideas led to the beloamphiphile designs of Scheme 2.

**Design of Azine-Based Beloamphiphiles.** Conjugated D–A systems were sought with modest dipole moments (2–4 D) along their long axes and with the propensity for high lateral intermolecular interactions. Placement of two acceptors with opposite polarity in the center of the molecules achieves the design goal of “dipole minimization.” This design element reduces or even eliminates through-conjugation in the ground state and has the overall effect that one-half of the molecule remains dipolar while the other half is rendered quadrupolar along the long axis. Williams pointed out the role of the high quadrupole moment of benzene in intermolecular bonding,<sup>28</sup> and our design employs arenes as “alignment units” and relies on the strengthening of lateral interactions with arene–arene interactions.

**Intra- and Interlayer Intermolecular Interactions.** The intermolecular interactions in the crystals depend on a variety of structural characteristics of the molecule (lengths, segments, twists, ...) and crystal structure (lateral and longitudinal offsets, interlayer angle, ...), and the various terms are correlated with each other. The matrix shown in Table 1 is useful to keep track of the types of interactions between the molecular fragments and of their correlation. The main body of the matrix provides an inventory of the interactions between two molecules. The segments of one molecule appear in column 1 (green) and the segments of the other in row 1 (blue) of Table 1. For the acetophenone azines the segments are head group X, para-disubstituted arene  $Ar_x$ , azine spacer Az, para-disubstituted arene  $Ar_y$ , and head group Y. Column 1 contains the molecule twice, and the top and bottom halves of the matrix describe parallel and antiparallel alignment,

**Table 1. Intermolecular Interactions Depending on Layer Polarity and Longitudinal Offset**

Intralayer Neighboring Interactions						Interlayer Neighboring Interactions	
	X = Hal	$Ar_x$	Az	$Ar_y$	Y = MeO	X	Y
X	X–X						X–Y
$Ar_x$	$Ar_x$ –X	$Ar_x$ – $Ar_x$					
Az	Az–X	Az– $Ar_x$	Az–Az				
$Ar_y$	$Ar_y$ –X	$Ar_y$ – $Ar_x$	$Ar_y$ –Az	$Ar_y$ – $Ar_y$			
Y	Y–X	Y– $Ar_x$	Y–Az	Y– $Ar_y$	Y–Y	Y–X	
X					X–Y	X–X	X–Y
$Ar_x$				$Ar_x$ – $Ar_y$	$Ar_x$ –Y		
Az			Az–Az	Az– $Ar_y$	Az–Y		
$Ar_y$		$Ar_y$ – $Ar_x$	$Ar_y$ –Az	$Ar_y$ – $Ar_y$	$Ar_y$ –Y		
Y	Y–X	Y– $Ar_x$	Y–Az	Y– $Ar_y$	Y–Y	Y–X	Y–Y

respectively. The columns on the right specify the interactions of the segments of the first two molecules with molecules of the same type in other layers (red).

The diagonal elements in Table 1 (shaded green and yellow) list the leading terms for the *intralayer* interaction energies  $E_{pp}$  and  $E_{app}$ , respectively, between parallel-aligned pairs or antiparallel-aligned pairs, respectively.

$$E_{pp} = E(X\sim X) + E(Ar_X\sim Ar_X) + E(Az\sim Az) + E(Ar_Y\sim Ar_Y) + E(Y\sim Y)$$

$$E_{app} = E(X\sim Y) + E(Ar_X\sim Ar_Y) + E(Az\sim Az) + E(Ar_Y\sim Ar_X) + E(Y\sim X)$$

The interaction between the spacers is about the same for both arrangements. The antiparallel alignment may occur in a variety of ways (Scheme 1), and in spite of all variability the alignment preference in essence depends on the difference of sums of terms between equal or different intermolecular bonding partners: Is  $E(Ar_X\sim Ar_X) + E(Ar_Y\sim Ar_Y)$  better than two  $E(Ar_X\sim Ar_Y)$ ? Is the sum of intralayer head group interactions  $E(X\sim X) + E(Y\sim Y)$  better or worse than two  $Y\sim X$  interactions? These questions can be answered qualitatively based on insights from the mixing of liquids. Pure pair interactions are usually favored over mixed pair interactions, and this tendency increases with the difference between the pure pair interactions:  $|E(X\sim X) - E(Y\sim Y)| = \epsilon$ . If the steric demands of X and Y are similar, formation of polar two-dimensional layers should thus be quite possible with beloamphiphiles for which the difference in lateral attraction (favors parallel) exceeds the difference in the dipole–dipole interaction (favors antiparallel).

The *interlayer* interactions (Table 1, right columns) between parallel and antiparallel BAMs, respectively, involve “nothing but mixed” or “mixed *and* pure” interactions, respectively. The intra- and interlayer interactions of any pair ( $X\sim X$ ,  $Y\sim Y$ ,  $X\sim Y$ ) obviously are not the same (geometry, anisotropy). Nevertheless, it becomes conceptually reasonable to state the hypothesis that the driving forces for layer formation and layer stacking are in opposition: Pure pair interactions favor parallel alignment in layers, while they reduce interlayer binding. Mixed interactions favor antiparallel alignment in layers but provide for better interlayer interactions. To solve the dipole alignment problem one must therefore pinpoint this balance: *Intralayer lateral interactions should be just large enough to make polar layers while still allowing polar stacking of the layers!*

## Prototypes and Design Refinements

**Synthesis and Crystallization.** Initially, we synthesized series of (RO,X)- and (RR'N,X)-azines  $Y\text{-Ph-MeC=N-N=CMe-Ph-X}$ . All of the (RR'N,X)-azines we prepared formed nonpolar crystals, and we published the structure of the (H<sub>2</sub>N,F)-azine as one such example.<sup>29</sup> Our first success came in 1995 with Chen's (MeO,Br)-azine:<sup>30</sup> Chen's azine forms perfect polar parallel beloamphiphile monolayers (PBAM, Figure 2) and the PBAMs stack with near-perfect polar alignment in the third dimension (Figure 3). In 2000 we reported the polar structures of the (MeO,Cl)-<sup>31</sup> and (MeO,I)-azines<sup>32</sup> (Figure 2), and recent efforts have focused on (RO,Hal)-azines with R = Et, Pr, ..., Dec, and Ph.<sup>33,34</sup> The beloamphiphile monolayers (BAMs) formed by the (EtO,Br)- and (*i*PrO,Br)-azines are shown in Figure 2, and the crystal structures of the two perfectly aligned (DecO,Br)- and (PhO,Br)-azines are illustrated in Figure 3. Overall, our work has resulted in the fabrication and structural characterization of 15 highly

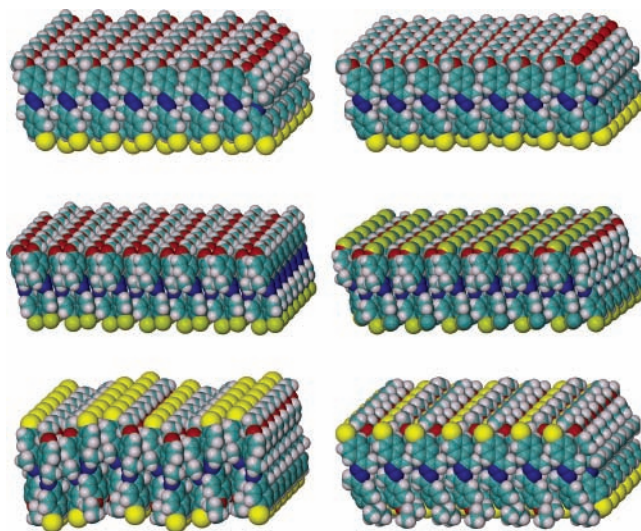


**FIGURE 2.** Parallel beloamphiphile monolayers of (MeO,Br)-azine (top left), (MeO,I)-azine (top right), and (MeO,Cl)-azine (center left) and antiparallel beloamphiphile monolayers of (MeO,Cl)-azine (center right), (EtO,Br)-azine (bottom left), and (*i*PrO,Br)-azine (bottom right).

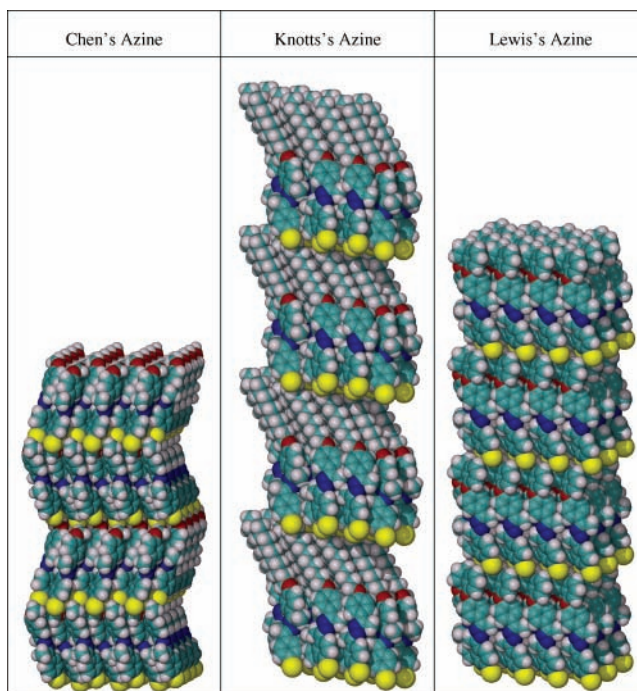


**FIGURE 3.** Polar order in (MeO,Br)-azine (left), (DecO,Br)-azine (center), and (PhO,Br)-azine (right).

parallel-aligned materials, and 7 of these crystals feature perfect polar order. Symmetrical azines allow for studies of  $X\sim X$  and  $Ar_X\sim Ar_X$  interactions, conformational properties, and electronic structures, and these azines are the essential reference to assess asymmetrization effects. We studied a variety of (X)<sub>2</sub>-azines, including X = CH<sub>3</sub>,<sup>35</sup> H,<sup>36</sup> Hal,<sup>37,38</sup> and others.<sup>39,40</sup>

The idea of dipole minimization has been central to our design, and this hypothesis was tested. We first showed that solid-state structures *cannot* be used for this analysis (even though this is common practice) because the effects of intramolecular charge transfer in ground

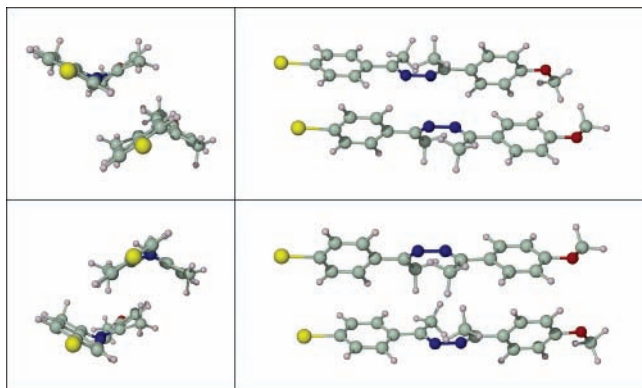


**FIGURE 4.** Double (ef|fe) T-contacts can be either “open” (top) or “closed” (bottom).

states are too small to manifest themselves in observable structural effects.<sup>41</sup> NMR studies (<sup>1</sup>H, <sup>13</sup>C) in a variety of solvents<sup>42,43</sup> and electronic structure analyses<sup>41</sup> firmly established that the electronic communication across the azine bridge is marginal in the acetophenone azines. Studies of symmetrical and unsymmetrical 2,5-diphenyl-2,4-hexadienes are underway,<sup>44</sup> and the results also will provide information on the concept of dipole minimization in azines.

**Lateral Offsets, Twists, and Double T-Contacts.** Azines provide for lateral offset (LatOS), that is, the local  $C_2$  axes of the para-disubstituted arenes do not coincide (Scheme 2). Lateral offset has major consequences for the crystal architecture, and these include the possibility for occurrence of double T-contacts.

Twists about the N–N and C–Ph bonds in acetophenone azines cause the arenes to be nearly perpendicular and enable each azine to engage in four “double T-contacts” of the (ef|fe)-type.<sup>45</sup> For a pair of diarenes, the (12|34)-abbreviation specifies for each arene whether it acts as “face” or “edge” in a T-contact, (12| refers to one molecule and |34) to the other, and it is understood that arene 1 interacts with arene 3 and arene 2 with arene 4. Each azine engages in two types of (ef|fe) contacts, and the “open” and “closed” contacts are exemplified in Figure 4. Open and closed contacts alternate in both layer directions. For these contacts to be most efficient, the molecules require a more or less constant cross-section along the long axis of the molecule.

**Unequal Lateral Offsets and Polarity Anisotropy.** The (ef|fe) interactions of a twisted molecule with lateral offset (*E*) with its neighbors (enantiomer *E'*) are *different in the two layer directions if the components of the lateral offset are unequal*. This is true for open and closed interactions alike. Should the components of the lateral offset happen to be equal, then the same interactions are possible in both layer directions. For unsymmetrical azines, there is every reason to expect unequal components of the lateral offset.

The (EtO,Br)- and (*i*PrO,Br)-azines form nonpolar anti-parallel beloamphiphile monolayers (APBAMs) but maintain polar sheets (Figure 2)! The polar sheets alternate in (*i*PrO,Br)-azine, whereas the crystal structure of (EtO,Br)-azine features polar double sheets. The sequence of the

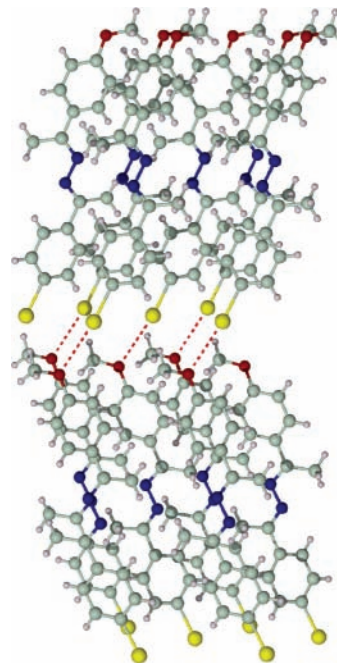


**FIGURE 5.** Crystals of (MeO,I)-azine feature perfect PBAMs and near-perfect parallel alignment in the stacking direction due to the directionality of interlayer halogen bonding.

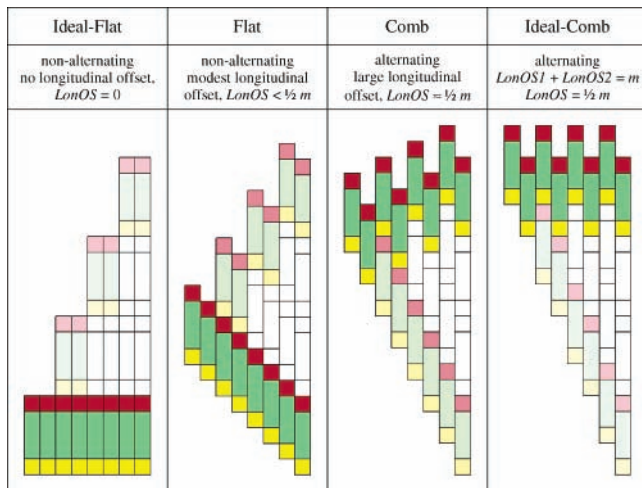
(MeO,Br)-, (EtO,Br)-, and (*i*PrO,Br)-azines thus exemplifies the gradual loss of polar alignment in one layer direction while maintaining polarity in the other. This polarity anisotropy is certainly enforced and possibly caused by the azines’ anisotropic lateral offsets.

**Interlayer Halogen Bonding and Layer Stacking.** The (MeO,Hal)-azines share a common crystal architecture but differ in details. Crystals of the (MeO,I)- and (MeO,Br)-azines contain *one* or *two* independent molecules, respectively, but both contain *one* kind of layer. The (MeO,Cl)-azine features *four* independent azines and *two* kinds of layers. Each (MeO,Cl) layer contains two independent molecules, much like a (MeO,Br)-azine layer, but only one (MeO,Cl) layer is perfectly aligned (Figure 2, left center) while the other layer (Figure 2, center-left) shows reproducible orientational disorder in one of the two molecules. The (MeO,Cl)-azine thus reveals in a compelling fashion the importance of interlayer halogen bonding in these crystals and also provides a rationale as to why we have not been able to crystallize the (MeO,F)-azine.

Halogen atoms (I, Br, Cl) engage in attractive interactions with N and O atoms, and this interaction is referred to as halogen bonding.<sup>46</sup> The directionality of interlayer halogen bonding (Figure 5) effects the stacking of the layers in the (MeO,Hal)-azine.<sup>3,43</sup> This insight suggested that replacement of the MeO group by the larger DecO or PhO groups and avoidance of directional halogen bonding might optimize the alignment in the stacking direction. We synthesized and crystallized the (DecO,Br)- and (PhO,Br)-azines and, indeed, Knotts’s and Lewis’s azines feature perfect polar order (Figure 3).

**Longitudinal Offsets, Stacking Options, and Lattice Energies.** The idealized displays of the beloamphiphile

**Scheme 3. Depending on the Magnitude of the Longitudinal Offset, *LonOS*, It Is Conceptually Advantageous To Discuss Nonalternating (“flat”) and Alternating (“comb”) Layers**



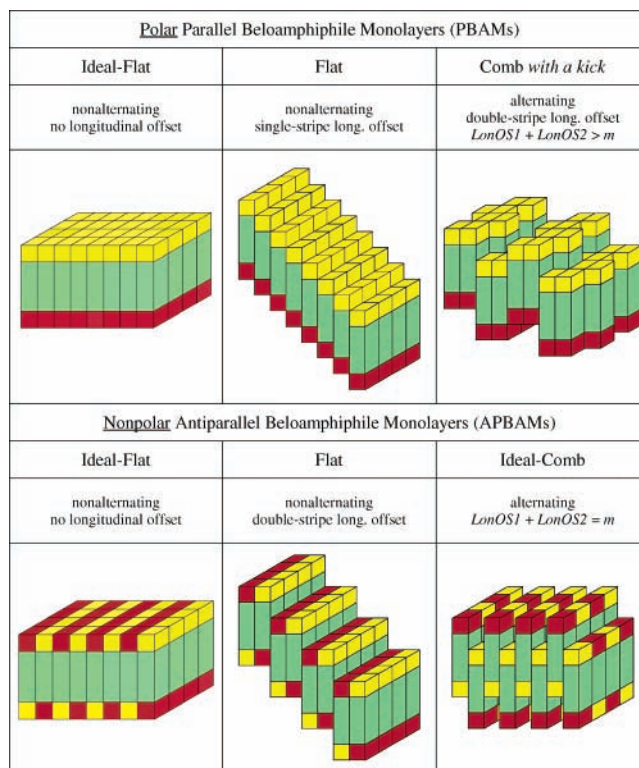
monolayers in Scheme 1 show all molecules exactly side by side. In reality, neighboring molecules may show longitudinal offset along the long molecular axis ( $LonOS$ ), there might be several offsets in one direction ( $LonOS\#$ ), and offset(s) in one layer direction ( $LonOS\#$ ) might be accompanied by offset(s) in the second direction ( ${}^2LonOS\#$ ).

If the longitudinal offset is modest, the layer retains its essential features and its surfaces remain “flat” (Scheme 3). As the longitudinal offset increases to reach or surpass one-half of the amphiphile’s length  $m$ , it becomes advantageous to consider comb-type layers. Comb-type BAMS can be constructed in various ways, and as with ideal-flat layers, ideal-comb layers stand out because the molecules’ long axes are perpendicular to the layer surfaces. The ideal-comb shown in Scheme 3 was constructed with alternating offsets  $LanOS1 = 2/5m$  and  $LanOS2 = 3/5m$ . Some relevant beloamphiphile monolayers with longitudinal offsets are shown in Scheme 4.

The longitudinal offsets in the polar azines are modest, and their layers are flat but not ideal-flat (Figure 2). The polar stacking of ideal-flat PBAMs *must* result in perfect polar alignment, while the stacking of flat PBAMs may give perfect or near-perfect polar alignment in the stacking direction, and the outcome depends on surface features. For example, halogen bonding is the likely cause for the near-perfect stacking of the flat layers of the (MeO,Br)-azine, while the flat layers of (DecO,Br)- and (PhO,Br)-azines stack with perfect polar order (Figure 3).

**Longitudinal Offsets and Synthons Variations.** As the longitudinal offset increases in a flat layer, interlayer interactions increase and lateral interactions change with regard to type and strength. Lateral X~X and Y~Y interactions decrease and new lateral synthons occur (e.g.,  $Ar_X \sim X$ ,  $Az \sim Ar_X$ , ..., shaded blue and orange in Table 1). As the offset increases even more, still other synthons occur (e.g.,  $Az \sim X$ , ..., shaded light blue and sand). To fully take advantage of this complexity requires recognition and characterization of all occurring synthons and their strengths and anisotropies.<sup>47</sup>

**Scheme 4. Types of Longitudinal Offsets in Polar PBAMs and Nonpolar APBAMs<sup>a</sup>**



<sup>a</sup> The flat and comb PBAMs, respectively, illustrate the (MeO,Hal)-azines and (*n*Bu,CN)-diphenyl, respectively. The APBAMs illustrate (*i*PrO,Br)-azine (flat) and (MeO,X)-azines (ideal-comb, X = NO<sub>2</sub>, CN).

As a first step to learning about  $Az \sim Ar_X$  interactions, we studied the quadrupole moment of formaldazine,  $H_2C=N-N=CH_2$ .<sup>48</sup> The component  $Q_{zz} = -25.6$  DÅ is largely due to the  $\pi$  system, compares on a per electron basis with  $Q_{zz}$  of benzene, and is representative of the quadrupole moment tensor component along the  $C_2$  axis of the azine bridge. Hence, this study suggests that azine moieties engage in strong quadrupole–quadrupole interactions with neighboring azine moieties and with arenes and that  $Az \sim Az$  and  $Az \sim Ar$  interactions are significant lateral synthons.

**Idioteloamphiphile Monolayers and Beloamphiphile Design.** Monolayers of the (Cl)<sub>2</sub>-, (Br)<sub>2</sub>-, (I)<sub>2</sub>-, and (MeO)<sub>2</sub>-azines are shown in Figure 6 and relevant IAM types in Scheme 5.

All (X)<sub>2</sub>-azines form structures with flat layers, and there are significant differences within the layers and their stacking.<sup>49</sup> The (I)<sub>2</sub>-azine forms flat IAMs, and their stacking is near perfect. While the (Cl)<sub>2</sub>- and (Br)<sub>2</sub>-azines realize the same IAM type, the IAMs of the (Cl)<sub>2</sub>-azine stack perfectly and the stacking in the (Br)<sub>2</sub>-azine is near perfect. The internal structures of the IAMs are particularly interesting in these two cases, and the packing of the halogens is emphasized in the right column of Figure 6. These are complex surfaces with double-stripe flat characteristics in one layer direction ( $LonOS \approx 2/5m$ ) and ideal-comb characteristics in the other layer direction (alternating offsets  ${}^2LonOS1 \approx 1/5m$  and  ${}^2LonOS2 \approx 4/5m$ ). The result is an “X-layer” that is *two* X-atoms deep,

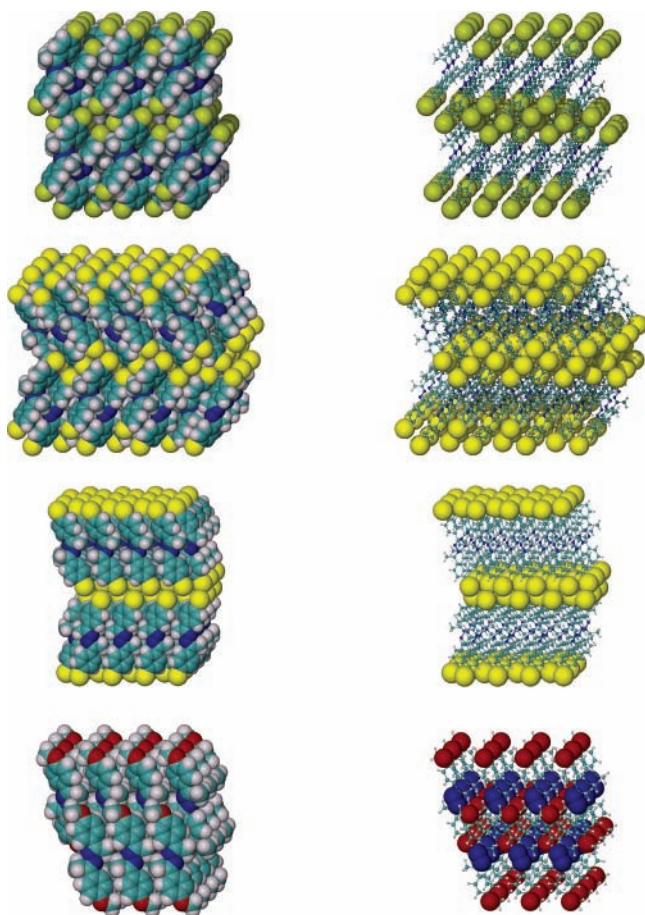


**FIGURE 6.** Interlayer interactions in idioteloamphiphile monolayers (top to bottom):  $(\text{Cl})_2^-$ ,  $(\text{Br})_2^-$ ,  $(\text{I})_2^-$ , and  $(\text{MeO})_2^-$ -azines.

**Scheme 5. Types of Longitudinal Offsets in IAMs<sup>a</sup>**

Idioteloamphiphile Monolayers (IAMs)		
Flat	Flat	Comb
nonalternating double-stripe long. offset	nonalternating single-stripe longitudinal offset $LonOS < 1/5\text{-}m$	alternating single-stripe longitudinal offset $LonOS = 2/3\text{-}m$
Ideal-Comb	Ideal-Flat	Ideal-Flat

<sup>a</sup> The two structures on the right feature longitudinal offset only in one layer direction and are ideal-flat in the other. The structure on the left features offsets in both layer directions. The illustrations show the structures of the  $(\text{Br})_2^-$  and  $(\text{Cl})_2^-$ -azines,  $(\text{I})_2^-$ -azine, and  $(\text{MeO})_2^-$ -azines, respectively.

and therefore, the interlayer interaction involves X atoms in *three* layers.

The idioteloamphiphile monolayer formed by the  $(\text{MeO})_2^-$ -azine is an excellent example of a comb-type layer with large longitudinal offset ( $LonOS > 3/5m$ ). Double T-contacts are realized in one layer direction but not in the other, and instead, lateral  $\text{Az}\sim\text{X}$  and  $\text{Ar}_\text{X}\sim\text{X}$  interac-

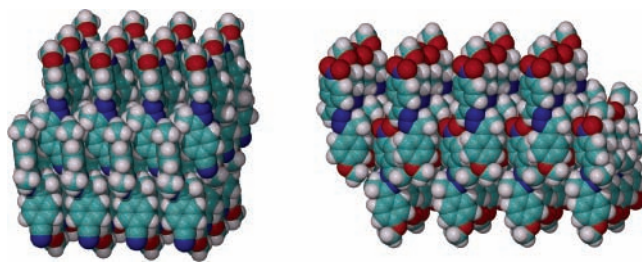


**FIGURE 7.** Antiparallel beloamphiphile monolayers (APBAMs) of  $(\text{MeO,CN})_2^-$ -azine (left) and  $(\text{MeO,NO}_2)_2^-$ -azine.

tions become important, lateral  $\text{X}\sim\text{X}$  interactions are avoided, and chain-forming (f|ef|e) contacts occur. In an (f|ef|e) contact, both arenes of one azine form T-contacts with arenes of two neighboring azines.

Future beloamphiphile designs will benefit from such insights about IAMs, but they will have to inform the designs with prudence. While it appears that the choice of halogens as head group was a particularly good one; in hindsight, one wonders whether one would have considered the MeO group as the polarity maker it turned out to be! The BAMs of Figure 1 are formed *in spite of* the MeO groups preference to avoid flat layers. We hope to gain more insight soon by studying the structures of the  $(\text{DecO})_2^-$ - and  $(\text{PhO})_2^-$ -azines.

**Antiparallel Beloamphiphile Structures and Beloamphiphile Design.** The  $(\text{CN})_2^-$ - and  $(\text{NO}_2)_2^-$ -azines are hardly twisted, and neither forms IAMs. Instead, the cyano-azine forms one-dimensional sheets with (f|ff|f) contacts, and the sheets are stacked with almost orthogonal orientations of the long axes in neighboring sheets. The crystal structure of the nitro-azine shows a related architecture and also relies on (f|ff|f) contacts. Would it be possible to build BAMs if one were to combine either one of these groups with the methoxy group?

We synthesized the  $(\text{MeO,CN})_2^-$ - and  $(\text{MeO,NO}_2)_2^-$ -azines, and their structures exemplify ideal-comb antiparallel beloamphiphile layers (Figure 7).<sup>30</sup> This is actually quite intriguing! The D–A systems are twisted even though the respective A–A systems are not, and these observations provide further corroboration of the azine's conjugation stopper capacity and the double T-contact's driving force to form BAMs. Nevertheless, the lateral interactions are not strong enough to form PBAMs. These crystals feature polarity alternation in both layer directions (checkerboard, Scheme 4, bottom-right) and complement the exposition of the APBAMs with polarity alternation in just one layer direction (e.g.,  $(i\text{PrO,Br})_2^-$ -azine).

**Biphenyl-Based Beloamphiphile Monolayers and Cyano Strategy.** Aside from the azines, a handful of molecular materials are known that crystallize with polar order. We cited these materials elsewhere<sup>3,45</sup> and pointed out that they vary greatly in their constitutions, they were all discovered by different groups, and none of these discoveries led to repetition, refinement, and/or conceptualization. Only the para-disubstituted biphenyls stand out in that two polar (X,Y)-biphenyls were published by two groups (Figure 8). Haase<sup>50</sup> reported the crystal structures of the  $(\text{RO,CN})_2^-$ -biphenyls (R = Me, Et, *n*Pr, *n*Bu), and

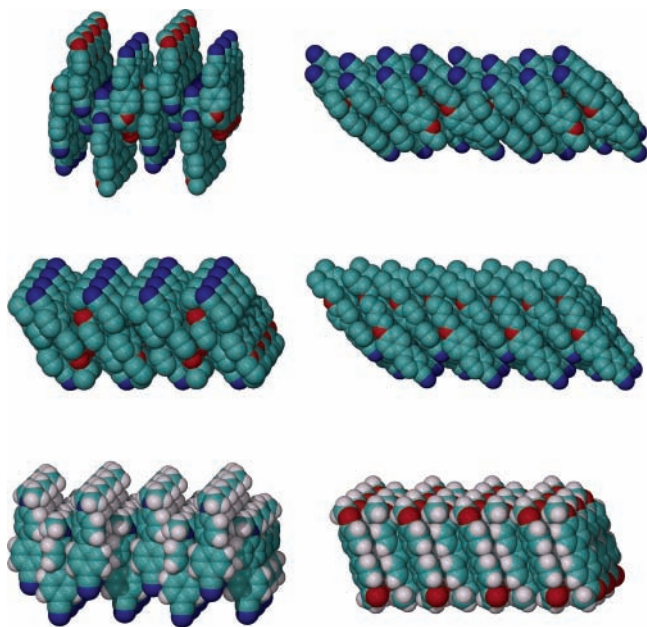


**FIGURE 8.** (MeO,CN)-Biphenyl (top left) features polar double sheets forming an ideal-comb BAM ( $LanOS1 + LanOS2 \approx m$ ), (EtO,CN)-biphenyl (top right) shows checkerboard polarity, and ( $nPrO,CN$ )-biphenyl (center left) contains ideal-flat polar sheets with alternating polarity and double-stripe longitudinal offset. Three diphenyls for polar PBAMs: ( $nBuO,CN$ )-biphenyl (center right), ( $Me_2N,CN$ )-diphenyl (bottom left), and (MeO,COMe)-biphenyl (AMB, bottom right).

crystals of ( $nBu,CN$ )-biphenyl are polar. In addition, Zyss<sup>51</sup> reported the polar structure of ( $Me_2N,CN$ )-biphenyl. Hence, it was a natural choice to apply the lessons learned from the azine studies to the engineering parallel-aligned polar biphenyls.

( $nBuO,CN$ )-Biphenyl exemplifies the PBAM-type “comb with a kick” (Scheme 5), and it is closely related to the IAM-type exemplified by the ( $Cl$ )<sub>2</sub>- and ( $Br$ )<sub>2</sub>-azines. Non-polar (RO,CN)-biphenyls feature intra- and interlayer, antiparallel R–CN $\cdots$ NC–R attractions with sideways offset. The RO size effects the spacing of the CN groups, and as RO grows in size, it apparently becomes better to form PBAMs with (more) offset-parallel (R–CN)<sub>2</sub> attractions. ( $Me_2N,CN$ )-Biphenyl forms polar, ideal-comb layers, and its structure is consistent with optimizing parallel-offset (R–CN)<sub>2</sub> contacts. If this conception is true and general, the polar (R<sub>n</sub>X,CN)-biphenyls might be first prototypes of a more general strategy to polar order that is focused on one dominant headgroup Y and the forcing of (more) intralayer Y~Y interactions (favors polar) instead of intra- and interlayer Y–Y interactions (favors nonpolar). Moreover, this conception of (RO,CN)-biphenyls provides information on azine studies as it suggests that (RO,CN)-azines might become polar as R increases (in spite of the non-polarity of (MeO,CN)-azine). This hypothesis is testable.

The biphenyl implementation of the “cyano-strategy” relies on weak interlayer interactions along the stacking direction of the polar PBAMs. A more general strategy for formation of biphenyl-based PBAMs would employ not just X and Y as polarity makers but also both head groups as interlayer synthons. Indeed, the crystal structure of (MeO,COMe)-biphenyl features polar stacking of flat polar

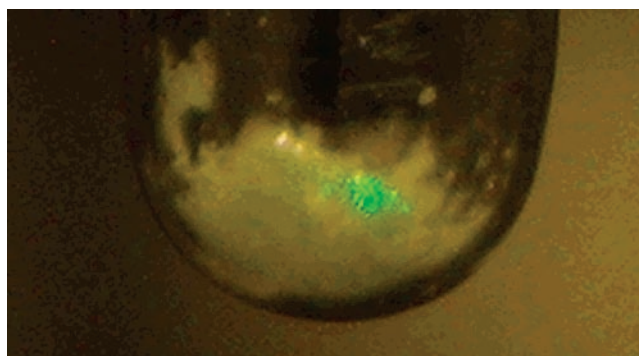


**FIGURE 9.** Nonlinear optical response of a microcrystalline powder sample of the polar-aligned (DecO,Br)-azine. The sample shines bright green (532 nm) at the target site of the IR laser (1064 nm).

layers and demonstrates a first success of this more general strategy.<sup>52</sup> It will be of interest to study (RO,Hal)-biphenyls.

## Conclusion

The polar crystals presented are ascendants of a new generation of highly anisotropic functional materials with perfect polar order. The astounding capabilities of such materials are illustrated in Figure 9: The nonlinear optical response of a microcrystalline powder sample of the polar (DecO,Br)-azine is visible even by the naked eye!<sup>34</sup>

The premise was taken from an essay<sup>53</sup> on software design, and similar thoughts apply to the rational design of materials. We clearly state our goals, describe and pursue rational strategies, and continuously examine and reassess all assumptions. While never guaranteed, success is almost inevitable when a rational approach is combined with somewhat adventurous and venturesome option selection during implementation. The rate of success has been accelerating with every success because of the benefits provided by the co-evolutionary spiral of design and deep prototype analysis. We have come to enjoy working on complex systems enormously; as complexity grows hardly anything remains impossible.

*We thank Dr. Charles Barnes for his skillful crystal structure analyses. This work was supported by the ACS Petroleum Research Fund (27139-ACA) and the MU Research Council and Board (URC-98-058, URC-99-069, RB #2358).*

## References

- (1) Patthy, L. *Protein Evolution*, 1st ed.; Blackwell Publishers: Oxford, U.K., 1999.
- (2) The Research Collaboratory for Structural Bioinformatics (RCSB) Protein Data Bank. <http://www.rcsb.org/pdb/>.
- (3) Glaser, R.; Knotts, N.; Wu, H. Polar Order in Crystalline Molecular Organic Materials by Rational Design. *Chemtracts* **2003**, *16*, 443–452.
- (4) In *Anisotropic Organic Materials-Approaches to Polar Order*; Glaser, R., Kaszynski, P., Eds.; ACS Symposium Series 798; American Chemical Society: Washington, DC, 2001; pp 97–111.
- (5) Berkowitz, M. L.; Smondyrev, A. M. Molecular Dynamics Simulation of Dipalmitoylphosphatidylcholine Membrane with Cholesterol Sulfate. *Biophys. J.* **2000**, *78*, 1672–1680.
- (6) Heller, H.; Schäfer, M.; Schulten, K. Molecular dynamics simulation of a bilayer of 200 lipids in the gel and in the liquid-crystal phases. *J. Phys. Chem.* **1993**, *97*, 8343–8360.
- (7) Kuzmenko, I.; Rapaport, H.; Kjaer, K.; Als-Nielsen, J.; Weissbuch, I.; Lahav, M.; Leiserowitz, L. Design and Characterization of



- Crystalline Thin Film Architectures at the Air-Liquid Interface: Simplicity to Complexity. *Chem. Rev.* **2001**, *101*, 1659–1696.
- (8) Weissbuch, I.; Popovitz-Biro, R.; Lahav, M.; Leiserowitz, L. Understanding and Control of Nucleation, Growth, Habit, Dissolution and Structure of Two- and Three-Dimensional Crystals Using 'Tailor-Made' Auxiliaries. *Acta Crystallogr., Sect. B* **1995**, *51*, 115–148.
- (9) Shoemaker, S. D.; Vanderlick, T. K. Intramembrane Electrostatic Interactions Destabilize Lipid Vesicles. *Biophys. J.* **2002**, *83*, 2007–2014.
- (10) Bagchi, B. Water Dynamics in the Hydration Layer around Proteins and Micelles. *Chem. Rev.* **2005**, *105*, 3197–3219.
- (11) Sokolov, V.; Mirsky, V. Electrostatic potentials of bilayer lipid membranes: basic principles and analytical applications. *Chem. Sensors Biosensors* **2004**, *2*, 255–291.
- (12) Menger, F. M. The structure of micelles. *Acc. Chem. Res.* **1979**, *12*, 111–117.
- (13) Chen, D.; Jiang, M. Strategies for Constructing Polymeric Micelles and Hollow Spheres in Solution via Specific Intermolecular Interactions. *Acc. Chem. Res.* **2005**, *38*, 494–502.
- (14) Silva, G. A.; Czeisler, C.; Miece, K. L.; Beniash, E.; Harrington, D. A.; Kessler, J. A.; Stupp, S. I. Selective Differentiation of Neural Progenitor Cells by High-Epitope Density Nanofiber. *Science* **2004**, *303*, 1352–1355.
- (15) Stupp, S. I.; LeBonheur, V.; Walker, K.; Li, S. K.; Huggins, K. E.; Keser, M.; Amstutz, A. Supramolecular Materials: Self-Organized Nanostructures. *Science* **1997**, *276*, 384–380.
- (16) Plant, A. L. Supported Hybrid Bilayer Membranes as Rugged Cell Membrane Mimics. *Langmuir* **1999**, *15*, 5128–5135.
- (17) Fuhrhop, J. H.; Helfrich, W. Fluid and solid fibers made of lipid molecular bilayers. *Chem. Rev.* **1993**, *93*, 1565–1582.
- (18) Lasic, D. D.; Needham, D. The "Stealth" Liposome: A Prototypical Biomaterial. *Chem. Rev.* **1995**, *95*, 2601–2628.
- (19) Fuhrhop, J.-H.; Wang, T. Bolaamphiphiles. *Chem. Rev.* **2004**, *104*, 2901–2938.
- (20) Jin, W.; Fukushima, T.; Niki, M.; Kosaka, A.; Ishii, N.; Aida, T. Self-assembled graphitic nanotubes with one-handed helical arrays of a chiral amphiphilic molecular graphene. *Proc. Natl. Acad. Sci.* **2005**, *102*, 10801–10806.
- (21) De Wall, S. L.; Barbour, L. J.; Gokel, G. W. Solid-state bilayer formation from a dialkyl-substituted lariat ether that forms stable vesicles in aqueous suspension. *J. Phys. Org. Chem.* **2001**, *14*, 383–391.
- (22) Sim, G. A. The Crystal Structure of 11-Amino-Undecanoic Acid Hydrobromide Hemihydrate. *Acta Crystallogr.* **1955**, *8*, 833–840.
- (23) Zabel, V.; Müller-Fahrnow, M.; Hilgenfeld, R.; Sängler, W.; Pfannemüller, B.; Enkelmann, V. L.; Welte, W. Amphiphilic Properties of Synthetic Glycolipids Based on Amide Linkages. II. Crystal And Molecular Structure of *N*-(*n*-Octyl)-D-Gluconamide, an Amphiphilic Molecule In Head-To-Tail Packing Mode. *Chem. Phys. Lipids* **1986**, *39*, 313–327.
- (24) Jeffrey, G. A.; Maluszynska, H. The Crystal Structure and Thermotropic Liquid-Crystal Properties of *N*-(*n*-undecyl)-D-gluconamide. *Carbohydr. Res.* **1990**, *207*, 211–219.
- (25) Masuda, M.; Shimizu, T. Multilayer structure of an unsymmetrical monolayer lipid membrane with a 'head-to-tail' interface. *Chem. Commun.* **2001**, 2442–2443.
- (26) Steiger, D.; Ahlbrandt, C.; Glaser, R. Crystal Potential Formula for the Calculation of Crystal Lattice Sums. *J. Phys. Chem. B* **1998**, *102*, 4257–4260.
- (27) Steiger, D.; Glaser, R. Lattice Sum Calculations for  $1/r^p$  Interactions via Multipole Expansions and Euler Summations. *J. Comput. Chem.* **2001**, *22*, 208–215.
- (28) Williams, J. A. The molecular electric quadrupole moment and solid-state architecture. *Acc. Chem. Res.* **1993**, *26*, 593–598.
- (29) Lewis, M.; Barnes, C. L.; Glaser, R. The supramolecular architecture of 4-aminoacetophenone (1-(4-fluorophenyl)ethylidene)hydrazone hydrate. Double T-Contacts and Extremely Low-Density Water Layers in a Mixed Azine. *Can. J. Chem.* **1998**, *76*, 1371–1378.
- (30) Chen, G. S.; Wilbur, J. K.; Barnes, C. L.; Glaser, R. Push-Pull Substitution versus Intrinsic or Packing Related N-N *Gauche* Preferences in Azines. Synthesis, Crystal Structures and Packing of Asymmetrical Acetophenone Azines. *J. Chem. Soc., Perkin Trans. 2* **1995**, 2311–2317.
- (31) Lewis, M.; Barnes, C. L.; Glaser, R. 4-Chloroacetophenone-(4-methoxyphenylethylidene) hydrazone. *Acta Crystallogr., Sect. C* **2000**, *56*, 393–396.
- (32) Lewis, M.; Barnes, C. L.; Glaser, R. Near-Perfect Dipole Parallel-Alignment in the Highly Anisotropic Crystal Structure of 4-Iodoacetophenone-(4-methoxyphenylethylidene) Hydrazone. *J. Chem. Crystallogr.* **2000**, *30*, 489–496.
- (33) Glaser, R.; Lewis, M.; Knotts, N.; Ratchford, J. Unpublished results.
- (34) Glaser, R.; Knotts, N.; Yu, P.; Li, L.; Chandrasekhar, M.; Martin, C.; Barnes, C. L. Perfect polar stacking of parallel beloamphiphile layers. Synthesis, structure, and solid-state optical properties of the unsymmetrical acetophenone azine DCA. *J. Chem. Soc., Dalton Trans.* **2006**, 2891–2899.
- (35) Chen, G. S.; Anthamatten, M.; Barnes, C. L.; Glaser, R. Polymorphism and Conformational C=N–N=C Bond Isomers of Azines: X-Ray Crystal and *ab Initio* Structures of Two Rotameric Structures of Methyl (*para*-Tolyl) Ketone Azine. *Angew. Chem.* **1994**, *106*, 1150–1152; *Angew. Chem., Int. Ed. Engl.* **1994**, *33*, 1081–1083.
- (36) Chen, G. S.; Anthamatten, M.; Barnes, C. L.; Glaser, R. Stereochemistry and Stereoelectronics of Azines. A Solid State Study of Symmetrical, (*E,E*)-Configured, *para*-Substituted (H, F, Cl, Br, CN) Acetophenone Azines. *J. Org. Chem.* **1994**, *59*, 4336–4340.
- (37) Lewis, M.; Barnes, C.; Glaser, R. The Crystal Structure of 4-Iodoacetophenone Azine. *J. Chem. Crystallogr.* **1999**, *29*, 1043–1048.
- (38) Glaser, R.; Murphy, R. F.; Sui, Y.; Barnes, C. L.; Kim, S. H. Multifurcated Halogen Bonding Involving Ph–Cl–H–CPh=N–R' Interactions and Its Relation to Idioteloamphiphile Layer Architecture. *CrystEngComm* **2006**, *8*, 372–376.
- (39) Glaser, R.; Chen, G. S.; Anthamatten, M.; Barnes, C. L. Comparative Analysis of Crystal Structures of (*E,E*)-Configured *para*-Substituted Acetophenone Azines with Halogen, Oxygen, Nitrogen, and Carbon Functional Groups. *J. Chem. Soc., Perkin Trans. 2* **1995**, 1449–1458.
- (40) Glaser, R.; Chen, G. S.; Barnes, C. L. Conjugation in Azines. Stereochemistry of Benzoylformate Azines in the Solid State, in Solution, and in the Gas Phase. *J. Org. Chem.* **1993**, *58*, 7446–7455.
- (41) Glaser, R.; Chen, G. S. Asymmetrization Effects on the Structures and Populations of the Ground State of Dipolar Donor-Acceptor Substituted Molecular Organic NLO Materials. *J. Comput. Chem.* **1998**, *19*, 1130–1140.
- (42) Lewis, M.; Glaser, R. The Azine Bridge as a Conjugation Stopper: An NMR Spectroscopic Study of Electron Delocalization in Acetophenone Azines. *J. Org. Chem.* **2002**, *67*, 1441–1447, 7168.
- (43) Glaser, R.; Chen, N.; Wu, H.; Knotts, N.; Kaupp, M.  $^{13}\text{C}$ -NMR Study of Halogen Bonding of Haloarenes. Measurement of Solvent Effects and Theoretical Analysis. *J. Am. Chem. Soc.* **2004**, *126*, 4412–4419.
- (44) Glaser, R.; Dendi, L. R.; Knotts, N.; Barnes, C. L. *Ab Initio* and Crystal Structures of (*E,E*)-1,4-Diphenylbutadiene: A New Type of Arene-Arene Double T-Contact and an Interesting Inter-Layer Cooperation Involving Diastereoisomeric Contacts. *Cryst. Growth Des.* **2003**, *3*, 291–300.
- (45) Lewis, M.; Wu, Z.; Glaser, R. Arene-Arene Double T-Contacts. Lateral Synthons in the Engineering of Highly Anisotropic Organic Crystals. Chapter 7 in ref 4.
- (46) Metrangolo, P.; Resnati, G. Halogen bonding: a paradigm in supramolecular chemistry. *Chem. Eur. J.* **2001**, *7*, 2511–2519.
- (47) Desiraju, G. R. The supramolecular synthon in crystal engineering. *Stimulating Concepts Chem.* **2000**, 293–306.
- (48) Glaser, R.; Lewis, L.; Wu, Z. Conformational Effects on the Quadrupolarity of Azines. An *ab Initio* Quantum-Mechanical Study of a Lateral Synthon. *J. Mol. Model.* **2000**, *6*, 86–98.
- (49) McBride, J. M.; Bertman, S. B.; Semple, T. C. Structural Effects on Surfaces within Layered Crystals. *Proc. Natl. Acad. Sci.* **1987**, *84*, 4743–4746.
- (50) Walz, L.; Paulus, H.; Haase, W. Crystal and molecular structures of four mesogenic 4'-alkoxy-4-cyanobiphenyls. *Z. Kristallogr.* **1987**, *180*, 97–121.
- (51) Zyss, J.; Ledoux, I.; Bertault, M.; Toupet, E. Dimethylaminocyanobiphenyl (DMACB): a new optimized molecular crystal for quadratic nonlinear optics in the visible. *Chem. Phys.* **1991**, *150*, 125–135.
- (52) Glaser, R.; Knotts, N.; Wu, Z.; Barnes, C. L. Dipole Parallel Alignment in the Crystal Structure of a Polar Biphenyl: 4'-Acetyl-4-Methoxybiphenyl (AMB). *Cryst. Growth Des.* **2006**, *6*, 235–240.
- (53) Parnas, D. L.; Clements, P. C. A rational design process: How and why to fake it. *IEEE Trans. Software Eng.* **1986**, *12*, 251–257.

AR0301633